

# Synthetic Undersea Acoustic Transmission Channels

Dale Green\*, Joseph Rice<sup>†</sup>

*\*Benthos, Inc., 49 Edgerton Dr., North Falmouth, MA 02556*

*<sup>†</sup>SPAWAR Systems Center, & Department of Physics, Naval Postgraduate School, Monterey, CA 93943*

**Abstract.** Achieving effective through-water acoustic digital signaling (telesonar) requires an ability to adaptively accommodate a complex and possibly time-varying acoustic channel. Variable combinations of noise, interference, multipath, and motion impair real-world telesonar channels. When considering any one of these factors individually, performance degradation may be predicted from theory. But the combination of these factors can confound our theoretical predictive capabilities. A computer simulation of the acoustic channel is useful for developing telesonar waveforms and modems. The simulation directly drives the modem receiver with a virtually propagated analog signal, enabling us to test the performance of the synthetic end-to-end telesonar link. We have observed a close correlation between simulation-based performance and observed performance in at-sea channels exhibiting similar characteristics. The fact that telesonar performance is now quite predictable in a wide variety of channels is due, in large measure, to the use of channel simulation. The simulation presented here does not rely on physical modeling of the channel. Rather, it is based on the combination of theoretical multipath models (e.g., a Rician channel) with rapidly time-varying impulse response functions, where the statistics are derived from at-sea experiments or governed by values derived from independent physics-based models (e.g., PC-SWAT, Bellhop, etc). Noise and other additive interference are combinations of theoretical and stored data, and range rate-induced compression and dilation are incorporated.

## INTRODUCTION

The achievement of practical underwater acoustic communications, or telesonar, owes much to the earlier development of terrestrial wireless communications. Indeed, the fundamental theoretical precepts of wireless communications apply equally well to telesonar, and the physical layer signaling techniques used for telesonar would be recognized in most communications textbooks. The primary difference between the two is the adjustments made to accommodate to the physical channel. In particular, telesonar deals with very limited signal bandwidths, with frequency-dependent fading caused by multipath, with long latencies, and with time-varying channel impulse response functions. These factors have forced the development of a relatively unique structure for the implementation of effective communications in the underwater acoustic channel.

A good example of the differences between telesonar and RF wireless communications is the use of power control in the RF world to enable multi-access communications. In the code division multiple access (CDMA) cell phone system used in the U.S., a base station maintains instantaneous links with many individual cell phones via a secondary channel unseen by the cell phone user. This link is used to control the transmitted power levels of all phones so that all primary signals are received at the base station with approximately equal power. This enables the use of a type of signal which has auto- and cross-correlation properties similar to those of uncorrelated, Gaussian, white noise. However, in the acoustic domain, several issues conspire to make such a network difficult to achieve:

mobile nodes at some distance from a base station may well move into quite different channels by the time a power control signal could be received from the base; furthermore, the very limited bandwidths and transducer systems currently available have to date prevented the development of full-duplex signaling.

Rapid temporal variations in the impulse response functions may severely constrain the use of phase coherent signaling but have markedly less impact on non-coherent signaling techniques. This fundamental issue with the physics of telesonar channels has been addressed with some success by the use of adaptive channel equalization, especially via the decision feedback equalizer (DFE) originally developed by Proakis [1]. However, there still are important, unresolved issues with channel equalizers which make their performance difficult to predict.

The tremendous variety of “real-world” telesonar channels, combined with the very real difficulty of obtaining sufficient physical information to fully characterize a given channel, has substantially constrained the ability of physics-based propagation models to predict the performance of telesonar systems. Even in those situations in which good physical characterization is available, the real-time computational burden required for physics-based modeling of high frequency, time-varying channels is considerable.

Our approach to telesonar simulation is to rely on statistics which describe: the (possibly) time-varying impulse response function of the channel; the character of the interference (both “noise” and discrete interferences); and certain properties of the communicating platform (e.g., range rate). These statistics may be obtained from physics-based propagation models (e.g., PC-SWAT, Bellhop, etc), or they may be obtained from pertinent at-sea experiments.

Our approach is to identify telesonar performance in statistically describable channels, and not to replicate any specific physical channel. Performance is based on metrics obtained from real telesonar modems with analog input provided by a simulator. In this way we test the end-to-end link as one system. We evaluate performance in well-understood, benign channels, then search for worst case channel conditions which “break” the modem.

## **SIGNAL DISTURBANCES**

The phenomena we discuss which disturb the transmitted signal are those which have been observed empirically as detracting in a substantial way from modem performance. In this paper we discuss modeling of the signal received over a complex multipath channel, representation of noise, modeling of discrete interferences and jammers, and constant velocity motion (range rate). There is no particular importance of ordering in the following descriptions. Indeed, on a specific modem, the importance of a particular channel characteristic is determined by the effect it has on modem performance: rapid temporal variation in the impulse response function may severely constrain the use of phase coherent signaling, but have virtually no impact on non-coherent signaling techniques.

## Modeling and Simulating The Acoustic Channel

### Modeling

In the following, we first describe the receipt of a perfectly observable signal, but we quickly recognize that empirical estimation of channel characteristics will be constrained by the nature of the signal probes we use. In particular, we would employ a broadband (but band-limited) pulse processed with a replica correlator to examine the (band-limited) approximation to the channel impulse response. This specifically limits the observation of those components of the impulse response which are temporally closer than approximately  $1/W$ , with  $W$  the pulse bandwidth.

The impulse response function describes the (possibly time-varying) temporal and spectral distribution of energy presented to a receiver by the channel. This function has been extensively studied [2,3], and it is not our purpose to replicate the detailed mathematical derivations that have been developed by others. We simply present our version of the received signal as follows. The received signal is ideally described as a collection of  $N$  amplitude-weighted, delayed versions of the transmitted signal  $s(t)$  with amplitude  $a_n(t)$  and delay  $\tau_n$ : For convenience, we assume that  $s(t)$  is analytic (1-sided spectrum).

$$r(t) = \sum_n a_n(t) s(t - \tau_n). \quad (1)$$

In eqn (1), we assume the following:

1.  $a_n(t)$  is a circular (complex) Gaussian random variable with zero mean and with power (variance)  $b_n^2 = E_a |a_n(t; \tau)|^2$ , where  $E_a$  is the expectation operator over the amplitudes for the  $n$ th path.
2.  $b_n^2$  is constant for the duration of a single transmission, although the complex nature of  $a_n(t)$  may change during that duration.
3. The delays  $\tau_n$  reflect theoretical predictions or at-sea observations of time spread. They are constant for the duration of a single transmission.

Because the path power is constant, the time-varying nature of the individual path amplitude is described by the (assumed) wide sense stationary coherence function of the path,  $\rho_n$ :

$$\rho_n(\Delta t) = E_a |a_n^*(t) a_n(t + \Delta t)|^2 / b_n^2 \quad (2)$$

We observe that  $\rho_n$ , being a coherence function, has a duality in the Fourier domain which may be interpreted as a power spectrum  $P_n(f)$  with integrated power equal to  $b_n^2$ . The effective bandwidth of  $P_n(f)$  is determined by the time difference at which  $\rho_n(\Delta t)$  drops to an agreed-upon value. We define  $B_n$  to be the (3-dB) bandwidth of this path, or the inverse of  $\Delta t$  for which  $\rho_n(\Delta t) = 0.75$ . We also observe that the Fourier transform of  $a_n(t)$  is  $A_n(f)$ , with the property that

$$P_n(f) = E_a |A_n(f)|^2. \quad (3)$$

Now, we assumed that  $a_n(t)$  was a Gaussian function, so  $A_n(f)$  is likewise Gaussian at every frequency component.

As an example, consider a condition in which we had observed a channel with two dominant paths, with a 4 ms temporal separation between them, a relative power of 1 and 0.5, respectively, and coherence times of 50 ms and 20 ms, respectively. The upper trace of Figure 1 shows a realization of the path weight  $|a_1(t)|$ , while the lower trace shows the sample auto-coherence properties of this weight. The dashed line in the upper plot indicates the duration of the signal relative to this weight. Figure 2 shows corresponding sample results for the second path. Note the width of the coherence function for the two paths, which correspond well with the specified (*a priori*) coherence time.

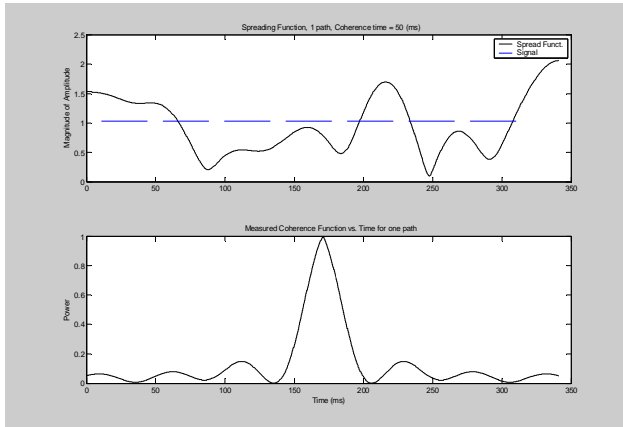


**Figure 1. A sample temporal weighting function reflecting a single path in an acoustic channel. the coherence time (75% confidence level) for this path is specified to be 50 ms.**

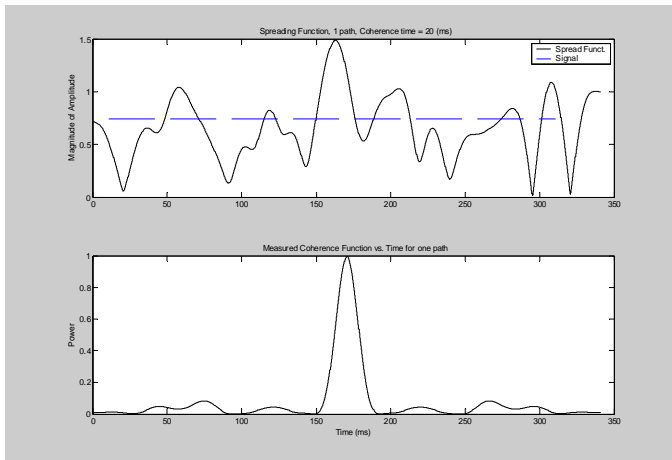


**Figure 2. A sample temporal weighting function reflecting a single path in an acoustic channel. The coherence time (75% confidence level) for this path is specified to be 20 ms.**

According to Eqn (1), the desired signal,  $s(t)$ , is independently multiplied by each of the weights, and the products are delayed according to the respective path delays, and the results summed. The upper plot of Figure 3 shows a sample waveform received over our example 2-path channel. A standard signal processing technique is to process this signal with a matched filter, the filter being a copy of the transmitted waveform. The lower plot of Figure 3 shows the output of such a matched filter. It is seen that this is a useful tool in

evaluating the gross characteristics of the channel: the delay between the two paths is accurate, and the relative powers are reasonably close to the specification.

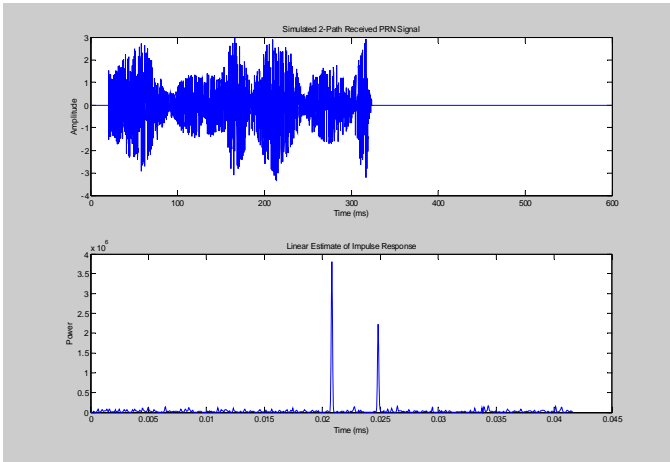


**Figure 3.** A PRN waveform received over a simulated 2-path channel (upper plot). The lower plot shows a classic matched filter output when the entire waveform is used as the filter.

We now consider the limitations we face in measuring and estimating these channel characteristics. In particular, the assumption implicit in eqn (1), that the received components of  $r(t)$  are observable cannot be justified or measured because the channel impulse response will be estimated via the correlation function of a band-limited waveform. The correlation function will have a temporal resolution approximately equal to the inverse of the waveform bandwidth,  $W$ . Thus, if several paths deliver the waveform with a temporal separation less than this resolution, the estimation will reflect a correlation among these arrivals. Furthermore, in a typical analysis system, the temporal sampling interval  $\delta t$  will be considerably less than  $1/W$ , so the information contained in each temporal sample of the correlation is itself correlated with adjacent samples. Thus we introduce yet another correlation function  $\kappa_{n,m}$  which describes the similarity between the  $n^{\text{th}}$  and  $m^{\text{th}}$  measured path components.

$$\kappa_{n,m} = E_{\tau} |a_n^* a_m|^2 \quad (4)$$

Our fifth assumption is thus

$$4. \quad \kappa_{n,m} = 0, \text{ if } |n-m| \delta t > 1/W$$

### *Simulation*

At this point we consider only the sampled received signal, with a sample rate  $f_s$  and a sample interval of  $\delta t = 1/f_s$ . The transmitted signal is of duration  $T$ , so there are  $K = T/\delta t$  samples. Thus, each path weight  $a_n(p\delta t)$  is represented by  $K$  samples, with  $1 \leq p \leq K$ , and the Fourier transform  $A_n(k\delta f)$  is represented by  $K$  frequency samples, with  $1 \leq k \leq K$ , with frequency spacing  $\delta f = f_s/K$ . We choose to ignore the expectation operator, and work with individual realizations, obtaining thereby estimates  $\tilde{a}_n(p\delta t)$  and  $\tilde{A}_n(k\delta f)$ . The intention is to fill the individual spectral bins of  $\tilde{A}_n(k\delta f)$  with independent, zero-mean,

complex Gaussian random numbers. We use unit variance Gaussian random numbers to fill the spectral bins lying under a window function, with the resulting spectrum normalized such that the integrated power is  $b_n^2$ . We use a Hanning window, with 3-dB power levels positioned at  $f_1$  and  $f_2$ . We now compute a realization of  $\tilde{a}_n(p\delta t)$  as the inverse Fourier transform of  $\tilde{A}_n(k\delta f)$ .

We have now computed all  $\tilde{a}_n(p\delta t)$  as independent random realizations. That is, every possible delay  $\tau_n$  reflects an independent path arrival. However, eqn (4) prescribes the requisite path-to-path temporal correlation. We approximate this correlation via application of a square root filter in the delay domain:

$$\tilde{a}_n(p\delta t) = (1 - (\kappa_{n,n-1})^{1/2}) \tilde{a}_n(p\delta t) + (\kappa_{n,n-1})^{1/2} \tilde{a}_{n-1}(p\delta t) \quad (5)$$

The correlation function  $\kappa$  is empirically determined.

### Comments and Observations

We obtain a path-dependent, time-varying temporal weighting function for every possible delay time via eqn (5). Each weight is of the same duration (or greater) as is the sampled signal,  $s(p\delta t)$ . Following eqn (1), therefore, we perform the multiplication  $\tilde{a}_n(p\delta t)s(p\delta t)$ . For all delay times  $\tau_n$  we delay the product and add it to all previous products. The result is the received signal,  $r(q\delta t)$ ,  $1 \leq q \leq (K + \max(\tau_n/\delta t))$ .

### *Estimation of Channel Characteristics*

Although the process described above for simulating a received waveform applies to any band-limited transmitted waveform, for purposes of estimation of channel characteristics, we use a pseudo-random (PRN) waveform for  $s(t)$ . A properly constructed PRN signal admits to separation into  $K$  components, each of which is effectively independent of all others. Each component may thus be used as a “sub-correlator” which is substantially immune to the presence of other components in the received waveform. We can take advantage of this feature by performing a correlation (matched filter) of the entire received waveform with each of the components. Because the temporal relationships of all components are known, the output of the sub-correlators can be arranged in a waterfall display, as shown in Figure 4. Here we observe the variations across time of the power measured at any given lag time. It is clear that this presentation reveals much more of the time-varying nature of the example channel than does the classical matched filter. Indeed, although the presentation in Figure 4 shows the magnitude-squared (power) of the sub-correlator outputs, the underlying complex outputs contain all of the information required to construct our channel model.

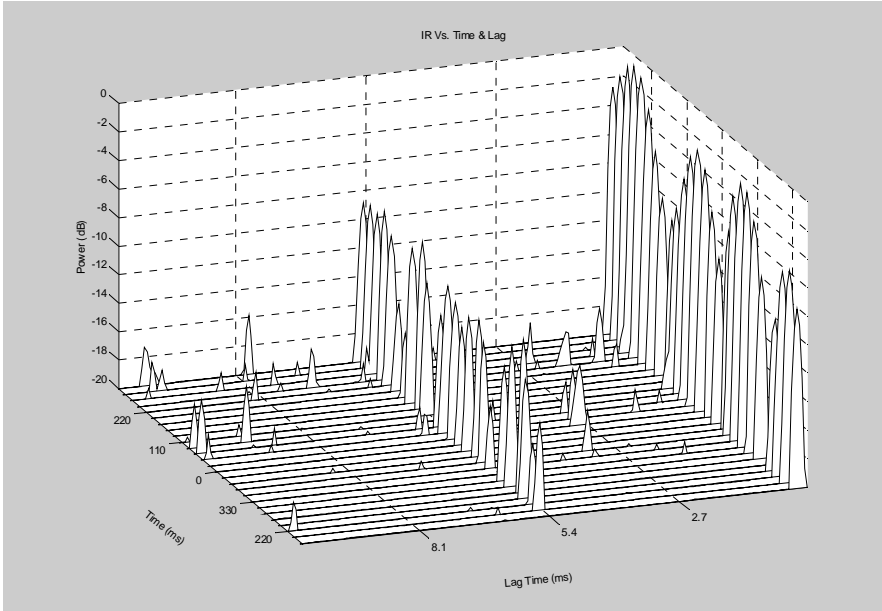


**Figure 4.** A waterfall display of the output of multiple sub-correlators, each a component of the transmitted waveform, each of which is used to process the entire received waveform.

### Modeling and Simulating Range Rate

Range rate is simply constant relative speed between a source and a receiver. The effect of range rate on a waveform is to cause a dilation or contraction in the temporal duration of the waveform. With a broadband waveform, the upper frequencies will shift more than will the lower frequencies, hence causing a contraction or dilation in frequency. It is only with a tonal waveform that contraction or dilation is equivalent to the so-called Doppler shift.

We consider an arbitrary waveform  $x(t; f_1; f_2; \varphi)$  which is a function of time ( $t$ ), a start frequency ( $f_1$ ), a stop frequency ( $f_2$ ), and a trajectory  $\varphi$  which defines the time-frequency path by which the waveform migrates from  $f_1$  to  $f_2$ . Time is described such that  $0 \leq t \leq T$ . A waveform subject to range rate may be modeled as:

$$x_\alpha = x(\alpha t; \beta f_1; \beta f_2; \varphi) \quad (6)$$

where  $\alpha$  is a constant multiplier, with  $\alpha \approx 1$ , and  $\beta$  is a function of  $\alpha$ , both to be defined.

The Fourier Transform of  $x(t)$  is  $X(f)$ , of  $x_\alpha(t)$  it is  $X_\alpha(f)$ , and it can be shown that

$$X_\alpha(f) = X(f/\alpha) \quad (7)$$

hence  $\beta = 1/\alpha$ . A useful description of  $\alpha$  arises from considerations of constant velocity motion:

$$\alpha \approx (1 + v/c) \quad (8)$$

where  $v$  is the relative velocity between a source and a receiver, and  $c$  is the propagation speed in the transmission channel. It is seen that  $\beta \approx (1-v/c)$ .

In the following we demonstrate a simple method for imposing compression/dilation on arbitrary (passband) waveforms. Let  $r(p\delta t)$  be any passband waveform with a carrier frequency of  $f_0$ , and an envelope function  $a(p\delta t)$ . There are  $K$  samples taken over  $T$

seconds. For convenience, we assume that  $r(p\delta t)$  is analytic, with baseband representation:

$$\hat{r}(\alpha p\delta t) = a(\alpha p\delta t)\exp(i2\pi f_0\alpha p\delta t), \quad 0 \leq p \leq (K-1)\alpha \quad (9)$$

From eqn (8) we have our compression/dilation factor  $\alpha$ . For every time value of  $(p\delta t)$  there is a corresponding value of  $(\alpha p\delta t)$  which reflects the compressed/dilated time equivalent. Note that, in eqn (9), in the absence of range rate we would have an exact baseband replica of the transmitted signal.

We now investigate an interpolative approach to imposing range rate effects on the baseband formulation of the “transmitted” waveform to give it the requisite characteristics of the received, distorted signal. First, we must interpolate the waveform envelope  $a(p\delta t)$  by a suitable amount to obtain  $a(n\delta t')$ . Our experience has been that a factor of  $M = 8$  is appropriate. That is, there are now  $0 \leq n \leq MK-1$  samples, each sample taken at  $M$ fs samples per second, with a new sample interval of  $\delta t' = \delta t/M$ . To compute the distorted envelope required by eqn (9), we compute an index  $n'$  for which

$$n' = \frac{\min}{n} [n - \alpha p\delta t / \delta t'], \quad (10)$$

$$\hat{y}(\alpha p\delta t) = a(n'\delta t') \quad (11)$$

Finally, recognizing the residual effect of speed on the carrier frequency,  $f_0$ , we multiply by the complex exponential to obtain the final “received” signal

$$\hat{r}(\alpha p\delta t) = \hat{y}(\alpha p\delta t)\exp(i2\pi f_0 p\delta t (\alpha - 1)) \quad (12)$$

Figure 5 shows spectral comparisons between a transmitted LFM signal, an analytical representation of the signal received from a 20 kt source, and the signal received with 20 kts, as produced by the numerical process. Note the offsets in frequency caused by the range rate, which is the same offset for the model and for the numerical techniques.

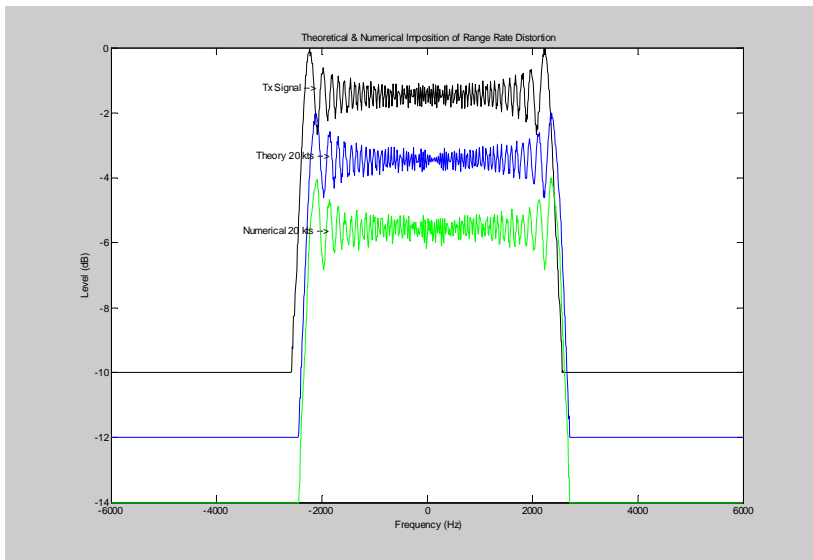


**Figure 5. Comparison of the Power spectra of the original transmitted LFM (upper trace), and the “received” signal perturbed by 20 kts of range rate. The middle trace reflects a theoretical model, while the third trace reflects a numerical imposition. They are virtually identical. The vertical offsets in the plots are included only to clarify the presentation.**

## **Modeling and Simulating Noise**

We have little to add to the decades-long development and understanding of additive noise, other than to describe our use of it in modem development. Whether we use artificially-generated noise or experimentally recorded noise, whether it is represented analytically or as a “real” component, we always pass the noise through a bandpass filter prior to adding it to any signal. The filter has approximately the same bandwidth as does the signal of interest. Our received signals (see eqn (1)) are always normalized to have unit power (variance) and the filtered noise is then normalized to have a power (variance) such that the ratio of signal power to noise power meets user-specified criteria for signal-to-noise-ratio (SNR). We note a consequence of this definition of SNR: because we maintain unit signal power, the SNR available on any individual channel path is reduced as the number of paths increases. This is especially detrimental for phase-coherent signaling in which an adaptive equalizer attempts to remove multipath influence from a time-varying channel: a path which is occasionally strong may at times be quite weak, and the overall response of the equalizer will be to treat the path signal as noise bursts.

## **CHANNEL SIMULATION (CHANSIM)**

Acomms performance is determined as much by acquisition, frequency alignment, and timing as it is by demodulation and decoding, and our experience is that these “preliminaries” are often the more demanding part of successful communications. We therefore have found it necessary to consider the effect of the channel (and platforms) on all aspects of the transmitted signal. In particular, we have found it necessary with our simulations to generate passband waveforms in an analog form and provide that directly into the output of the preamplifier of our modem receiver. We supply a few tens of seconds of “interference only” prior to the waveform to test the entire receiver, especially with regard to the automatic gain control (AGC) and false alarm performance.

Benthos has received funding from the US Navy via several modem-related programs dating back to 1998 for the purpose of developing a simulator adequate to meet the needs of modem development. This channel simulator (CHANSIM) is a MATLAB-based, GUI-driven, real-time emulation of real-world acoustic channels. It provides for most recognized effects of the channel, using statistical characteristics to control the realizations, which are converted via a digital -to-analog converter to a voltage signal which can drive the entire modem. Although the intended use of CHANSIM is for modem development, any band-limited waveform may be used as a “transmitted” signal. As such, the simulator is valid for sonar applications as well as telesonar applications.

CHANSIM has many features both to characterize the channel and to control the flow of the simulation. Table 1 lists the settable channel and control features of CHANSIM.

**Table 1. CHANSIM Channel Characteristics & Simulation Control**

Noise Types 1. band-limited AWGN 2. stored noise files from experiments, appropriately bandlimited & resampled to match the signal band 3. No noise	Signal-to-noise ratio number of realizations Waveform basebanding & decimation bandwidth control sample rate control
Interference Types 1. tonals, impulses 2. partial-band, short-term noise 3. recorded animal sounds (sea lions, whales, etc.) 4. External (stored files) waveforms (e.g., for multi-access interference)	External triggers Range rate to +/- 40 kts
Impulse response function characterization 1. manual entry (via cursor/mouse) 2. theoretical (Rayleigh, Rician, etc.) 3. from stored statistics, especially for time-varying channels	Analysis and plotting tools 1. spectrogram 2. magnitude 3. power spectrum 4. matched filter 5. plot individual impulse response realizations

## CONCLUSIONS

There are two basic portions of a waveform used for acoustic communications: acquisition/alignment/timing components, and the modulated signal. In most practical situations the two cannot be separated when evaluating performance of a modem. We have developed a real-time simulator which tests a modem for most of the observed influences of the acoustic channel. Those influences are described by statistical parameters, which can be obtained from physics-based propagation models, or from at-sea experiments. Although the simulation incorporates many channel characteristics, the two addressed in this paper reflect the modeling of time-varying impulse response functions, and the simulation of platform range rate as it affects an arbitrary waveform.

## REFERENCES

- [1] M. Stojanovic, J.A. Catipovic, J.G. Proakis, "Adaptive multi-channel combining and equalization for underwater acoustic communications," *J. Acoustic. Soc. Amer.*, vol 94, pp.1621-1631, 1993
- [2] P. Bello, "Characterization of randomly time-variant linear channels," *IEEE Trans. Commun. Syst.*, vil . CS-11, pp. 360-393, 1963
- [3] R. Kennedy, *Fading Dispersive Channels*, New York: Wiley, 1969